Metal-organic framework MIL-101(Cr) based mixed matrix membranes for esterification of ethanol and acetic acid in a membrane reactor

Óscar de la Iglesia* [1], Sara Sorribas [2], Eduardo Almendro [2], Beatriz Zornoza [2], Carlos Téllez [2], Joaquín Coronas [2]

[1] Centro Universitario de la Defensa Zaragoza, Academia General Militar, 50090 Zaragoza, Spain.

[2] Department of Chemical and Environmental Engineering and Instituto de Nanociencia de Aragón (INA), Universidad de Zaragoza, 50018 Zaragoza, Spain.

* Corresponding author. Tel: +34 976 73 98 33. E-mail: oiglesia@unizar.es.

ABSTRACT

Mixed matrix membranes (MMMs) based on the polyimide Matrimid® (PI) with metal-organic framework (MOF) MIL-101(Cr) as porous nanostructured filler were synthesized and applied as separation element in a membrane reactor to carry out the esterification of acetic acid with ethanol. The MMMs were characterized by techniques including X-ray diffraction, IR spectroscopy and scanning electron microscopy. In order to compare the performance of MIL-101(Cr)-PI MMMs in the membrane reactor, pure PI and HKUST-1-PI membranes were also used. MMMs provided a better reactor performance than the bare PI membrane because of the increase in permeability associated to the presence of MOF as filler. The PI membrane reactor barely achieved the same conversion as a fixed bed reactor, while the MIL-101(Cr)-PI membrane showed a reactor performance similar to that of the HKUST-1-PI membrane with higher stability, as confirmed by membrane characterization after the reaction experiments.

KEYWORDS

Mixed matrix membranes; Metal organic framework; Esterification; Membrane reactor; Pervaporation.

1. Introduction

Esters are important chemicals for several processes related to the manufacture of foods, cosmetic products, medicines and solvents [1]. They can be obtained by direct esterification between an alcohol and a carboxylic acid, a process which has attracted the attention of many researchers in recent decades. Moreover, the development of biodiesel has increased the interest in the esterification reaction, since it can be produced not only by transesterification of fatty acids, but also by direct esterification of different organic acids with methanol to obtain products such as methyl oleate [2] or methyl laurate [3].

An acid catalyst is required in esterification reactions to donate protons for the autoprotolysis of the carboxylic acid. Although homogeneous catalysts such as inorganic [4] or organic acids [5] have been used for this purpose, heterogeneous catalysts are preferred in order to avoid problems related with their separation or the corrosion of devices.

As esterification occurs, water is produced as a byproduct, causing hydrolysis of the ester up to a point at which thermodynamic equilibrium is reached. In order to exceed equilibrium conversions, an excess of alcohol has traditionally been used [6], given that the limiting step of the reaction is the attack of the carboxylic group by the alcohol. Nevertheless, this requires a further separation of the alcohol, thus increasing operation costs. Another alternative is the separation of water from the reaction medium, which can be carried out by means of reactive distillation and pervaporation processes [7]. Pervaporation of water presents some advantages in comparison with reactive distillation since it is independent of the volatilities of reactants and products. Furthermore, it has lower energetic costs given that only permeated compounds are evaporated [8].

A membrane reactor combining a membrane selective towards water and a heterogeneous catalyst is an excellent reactor configuration for carrying out esterification reactions, improving conversions and reducing costs. There are many studies of pervaporation coupled with esterification in the literature, with different catalysts and membranes. Even though zeolites have been used [9, 10] as catalysts in recent years, these have been displaced by ionic exchange resins because of their higher activity, as reported by the use of Amberlyst 15® [11-16], Amberlyst 131® [17] or the 002CR acid ion exchange resin [18] as catalyst.

Different types of membranes have been applied for esterification. Among the zeolitic membranes, with high mechanical, thermal and chemical stability, ZSM-5 [19], mordenite [12], sodalite [20] and zeolite T [18] membranes have been used. Polymeric membranes stand out for their high selectivity, low cost and easy preparation [21], in spite of their lower capacity to withstand reaction conditions. The number of works reporting the use of polymeric membranes is extensive: Korkmaz et al. [22] carried out the esterification of acetic acid and isobutanol using polydimethyl-siloxane (PDMS), poly(vinyl alcohol) and commercial Nafion 117, PERVAP 1201, and PERVAP 2216 membranes. Figueiredo et al. [13] and Lu et al. [23] produced ethyl acetate in a membrane reactor with commercial PERVAP 1000 and poly(vinyl alcohol) membranes, respectively. Rathod et al. [24] reported the reaction between propionic acid and isopropyl alcohol with a poly(vinyl alcohol)-polyether sulfone composite membrane. Finally, commercial PERVAP 2201 membrane has been used for the production of n-Butyl acrylate [17] and ethyl lactate [15].

Mixed matrix membranes (MMMs) composed of a homogeneous dispersion of porous fillers embedded within a membrane polymer matrix were developed to improve the performance of bare polymeric membranes. MMMs combine the high molecular sieving and sorption properties of molecular sieves with the desirable mechanical and processing properties of polymers. MMMs have been extensively used for the dehydration of water-organic mixtures by means of pervaporation. MMMs using zeolite ZSM-5 [25], zeolite H-ZSM-5 [26], zeolite A [27], carbon nanotubes [28, 29], mesoporous SBA-15 [30] and MCM-41 [31] as fillers have been studied, achieving higher selectivities and/or fluxes than those of pure polymer membranes.

Metal-organic frameworks (MOFs) are porous crystalline materials with high specific surface area and adsorption capacity. They also have properties of molecular sieving, flexibility, and versatility of functionalization if the appropriate organic ligand is chosen. Because of their inorganic–organic nature, they have better compatibility with the polymer phase than other fillers [32]. The combination of MOF crystals with a polymer in the form of a MMM has been widely studied for gas separation applications [33-35]. Regarding pervaporation, MMMs composed of chitosan and ZIF-7 [36], polyimide Matrimid® 5218 and ZIF-8 [31], Matrimid® 5218 and HKUST-1 [16] or polydimethyl-siloxane (PDMS) and ZIF-71 [37] have been applied for the separation of water/ethanol mixtures. Dehydration of isopropanol has also been carried out by using MMMs of poly(vinyl alcohol) and ZIF-8 [38], and polyimide P84 and ZIF-90 [39]. Finally, MMMs comprising polymethyl-phenylsiloxane (PMPS) and ZIF-8 have also been used for dehydration of isobutanol [40].

In spite of the number of works reporting separation of water by pervaporation using MMMs, there is a lack of studies concerning the application of MMMs in membrane reactors. Zeolite inorganic fillers, e.g. sodium alginate with zeolite beta [41] and with zeolite 4A [42], have mainly been used to exceed the thermodynamic equilibrium in the production of ethyl acetate with the sulfonated cation exchange resin Dowex-50 as catalyst. To the best of our knowledge, our previous work [16] is the only study to have dealt with pervaporation coupled with esterification using a MOF based MMM, made of the commercial polyimide Matrimid® 5218 and HKUST-1 as filler.

The objective of this work is to study the preparation of MMMs based on commercial Matrimid® 5218, using MOF MIL-101(Cr), a crystalline mesoporous material with inner free cage diameters up to 34 Å and pore aperture windows up to 16 Å, as filler and their application for the esterification of ethanol and acetic acid in a membrane reactor. In order to evaluate our results, these MMMs were compared with those of Matrimid® 5218 and HKUST-1. MIL-101(Cr) based MMMs have already been synthesized with polysulfone [34, 43] and also with polyimide Matrimid® [44] as polymers and tested for the separation of gases. Finally, MMMs based on MIL-101(Cr) should provide selectivity for water separation due to their hydrophilicity [45] and stability in water [34].

2. Materials and Methods

2.1. Synthesis of metal-organic frameworks (MOFs)

For the synthesis of MIL-101(Cr), 0.5 g of $CrCl_3 \cdot 6H_2O$ and 0.45 g of terftalic acid (98%, Sigma-Aldrich) were dissolved in 26 mL of distilled water [46]. After mixing, the solution was maintained for 30 min at 180 ^{o}C in a microwave oven. The solid was separated by centrifugation and washed with water. Then, synthesized MOF was activated with N,N-dimethylformamide, DMF (99.8%, Sigma-Aldrich) at 120 ^{o}C overnight and thereafter with methanol for 12 h under reflux. Finally, MIL-101(Cr) was dried at 100 °C overnight.

The synthesis of HKUST-1 was carried out according to the procedure described by Wee et al. [47]. For this purpose, 1.2 g of $Cu(NO_3)_2 \cdot 2.5H_2O$ (98%, Alfa Aesar) and 0.6 g of benzene-1,3,5-tricarboxylic acid (BTC, 98%, Alfa Aesar) were dissolved in 20 mL of ethanol (analytical grade, Scharlau). The solution was stirred for 24 h at room temperature and the final product was collected by centrifuging twice with distilled water and once with ethanol, and dried at 100 °C overnight.

2.2. Preparation of mixed matrix membranes (MMMs)

MIL-101(Cr) or HKUST-1 based MMMs were prepared as follows. Firstly, 4.5 g of chloroform and the required amount of MOF to have the desired loading (20-30 wt%) were mixed for 20 min in an ultrasound bath and stirred overnight to achieve a complete dispersion of the solid. Afterwards, the corresponding amount of polyimide Matrimid® 5218 (hereafter called PI), kindly supplied by Huntsman Advanced Materials (Matrimid 5218 US), was added and the mixture was stirred for 24 h. The preparation method was the same for both MIL-101(Cr) and HKUST-1 MMMs. In the case of pure PI membranes, only the second step was carried out. Note that in all cases the total amount of filler and polymer was 0.4 g and the weight proportion of solvent:(filler+polymer) mixture was maintained constant at 91:9.

The suspension was then treated in an ultrasound bath with sonicating/mixing during three intervals of 15 min, cast on a flat glass plate and then left overnight partially covered to slow down the natural evaporation of the solvent under ambient conditions. Once dried at room temperature, the films were treated at 180 °C for 24 h in a vacuum oven (10 mbar) in order to remove the remaining solvent.

2.3. Characterization

Nitrogen adsorption isotherms of MIL-101(Cr) powder were measured at 77 K using a Micromeritics Tri Star 3000 analyzer. Prior to the analysis, samples were outgassed with a heating rate of 10 °C/min until 110 °C for 8 h. The BET (Brunauer-Emmett-Teller) specific surface area was determined from the nitrogen adsorption–desorption isotherms.

The MIL-101(Cr) powders and MMMs were observed by scanning electron microscopy (SEM) using an Inspect F50 model scanning electron microscope (FEI). For sample preparation, the membranes were immersed in liquid nitrogen and then fractured. The powder and membrane samples were mounted on carbon tape and coated with platinum using a sputter coater.

To confirm the MIL-101(Cr) powder structure and its stability after dispersion in the polymer, the MOFs and the MMMs were analyzed by X-ray diffraction (XRD). This analysis was carried out at room temperature with a D-Max Rigaku diffractometer with a copper anode and a graphite monochromator to select Cu-Kα1 radiation (λ = 1.5418 Å).

Thermogravimetric analyses (TGA) were conducted using a Mettler Toledo TGA/SDTA 851e system. Samples (about 5 mg) were placed in70 mL pans and then heated in air flow up to 750 °C at a heating rate of 10 °C/min.

The ATR-FTIR (attenuated total reflection Fourier transform infrared spectroscopy) characterization was performed using a Bruker Vertex 70 FTIR spectrometer equipped with a deuterated triglycine sulfate detector and a Golden Gate diamond ATR accessory. Spectra were recorded in the 4000–600 cm^{-1} wave number range with an accuracy of 4 cm^{-1}.

The water uptake of the membranes, sometimes described in the literature as the "degree of swelling" [30], was determined in water at 45 °C. Before the experiment, the membrane sample was dried at 100 °C for 3 h and weighed (W_{dry}, in the 50–80 mg range). Then the membrane was immersed in water for 20 h, and afterwards the fully swollen membrane was wiped with tissue paper and weighed again (W_{wet}). The water uptake was calculated by Eq. (1).

$$Water\ uptake\ (\%) = \frac{W_{wet} - W_{dry}}{W_{dry}} \cdot 100 \quad (1)$$

To check the stability of the MMMs, several of the above mentioned characterization techniques were applied after the esterification experiments. Furthermore, the MMMs were submitted to an experiment of leaching in which a piece of MMM was put in contact with a liquid mixture containing acetic acid (99%, Alfa Aesar), ethanol (analytical grade, Scharlau), ethyl acetate (99.7%, Sigma-Aldrich) and water with a composition corresponding to a conversion of 64% (steady state conversion obtained in a fixed bed reactor at 70 °C). The weight ratio between membrane and liquid was the same as in an esterification experiment with a feed of 0,046 g/min that lasted for 4 days. After this leaching experiment, the membranes were analyzed by TGA to determine the amount of metal present in the membrane.

2.4. Esterification experiments

Two reactor configurations were used: membrane reactor (MR) and fixed bed reactor (FBR).

In the MR experiments, the esterification reaction was carried out in a stainless steel permeation module using the prepared flat membranes with an effective area of 12 cm^2. The module was placed in an oven to provide an operation temperature of 70 °C. 2 g of ionic exchange resin Amberlyst 15® (hydrogen form, Fluka analytical) was put in the module as catalyst and 0.05 mL/min of an acetic acid-ethanol equimolar mixture was fed to the module at room temperature and with an overpressure of 0.2 bar. The retentate was collected on a glass deposit immersed in a water bath for cooling and avoiding further reaction. The permeate side was evacuated using a vacuum pump providing a pressure lower than 10 mbar, and the permeate vapor was condensed in a glass cold trap immersed in liquid nitrogen. The feed, retentate and permeate were weighed to determine the membrane flux and analyzed

with a gas chromatograph (Agilent Technologies, 7820A) equipped with a PORAPAK Q80/100 column using TCD and FID detectors.

In case of FBR experiments, a non-porous disk was placed in the permeation module instead of the membrane, and no permeate was obtained.

The ratio between the mass flow of reactants and the mass of catalyst was characterized by the weight hourly space velocity (WHSV). Conversion was calculated by Eq. (2):

$$X\ (\%) = \frac{\dot{n}_i^{inlet} - \dot{n}_i^{outlet}}{\dot{n}_i^{inlet}} \cdot 100 \quad (2)$$

where $\dot{n}_i^{inlet}$ is the molar flow of the reactant (either ethanol or acetic acid) fed to the reactor and $\dot{n}_i^{outlet}$ is the sum of the molar flow of the reactant in permeate and retentate. Permeate fluxes (J_i, kg·m^{-2}·h^{-1}) of the components were calculated by the following equation:

$$J_i = \frac{\dot{m}_i}{A} \quad (3)$$

where $\dot{m}_i$ is the mass flow of the component i in the permeate and A is the surface of the membrane.

Finally, the separation factor ($\alpha_{prod/react}$) between products and reactants was calculated by Eq. (4). This parameter gives a relation between the amount of products permeated (and removed from the reaction medium) and that of reactants lost with the permeate.

$$\alpha_{prod/react} = \frac{(Y_{EtAc}+Y_{H2O})\big/(Y_{HAc}+Y_{EtOH})}{(X_{EtAc}+X_{H2O})\big/(X_{HAc}+X_{EtOH})} \quad (4)$$

In this equation, Y_i and X_i are the mass fraction of each component in the permeate and retentate, respectively.

3. Results and discussion

3.1. Filler characterization

The XRD diffractogram of synthesized MIL-101(Cr) is shown in Fig. 1. The diffraction peaks are consistent with those of the simulated pattern obtained with Mercury 3.3 software using the corresponding CIF file [48]. The broad peaks of the XRD patterns are related to the nanoparticle size of the MIL-101(Cr) sample, corroborated by SEM (Fig. 2).

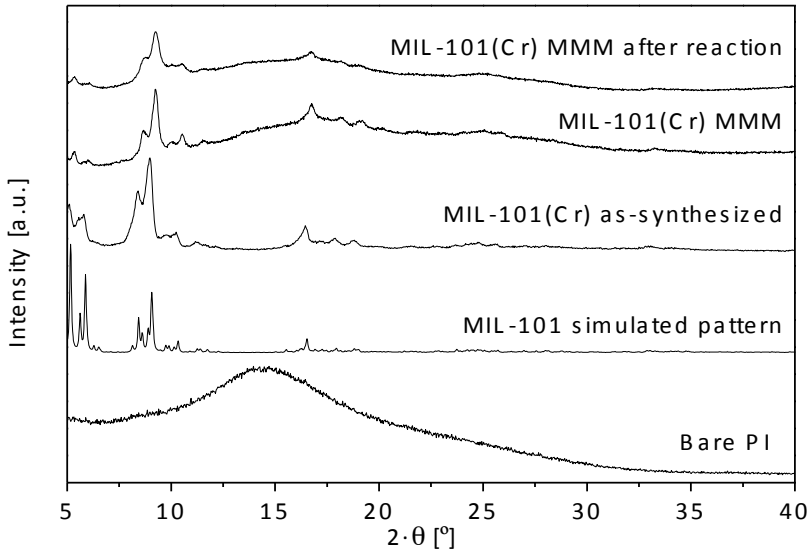

Figure 1. XRD patterns of bare PI membrane, MIL-101 simulated pattern, as-synthesized MIL-101(Cr) powder and the corresponding MIL-101(Cr) MMMs: as-synthesized and after esterification reaction.

Fig. 2a shows a SEM image of the synthesized MIL-101(Cr). As can be seen, a narrow distribution of particle size was obtained, with an average particle size of 58.9 ± 9.2 nm calculated from averaging 20 specimens. This particle size is similar to previously reported values of MIL-101(Cr) particles [46].

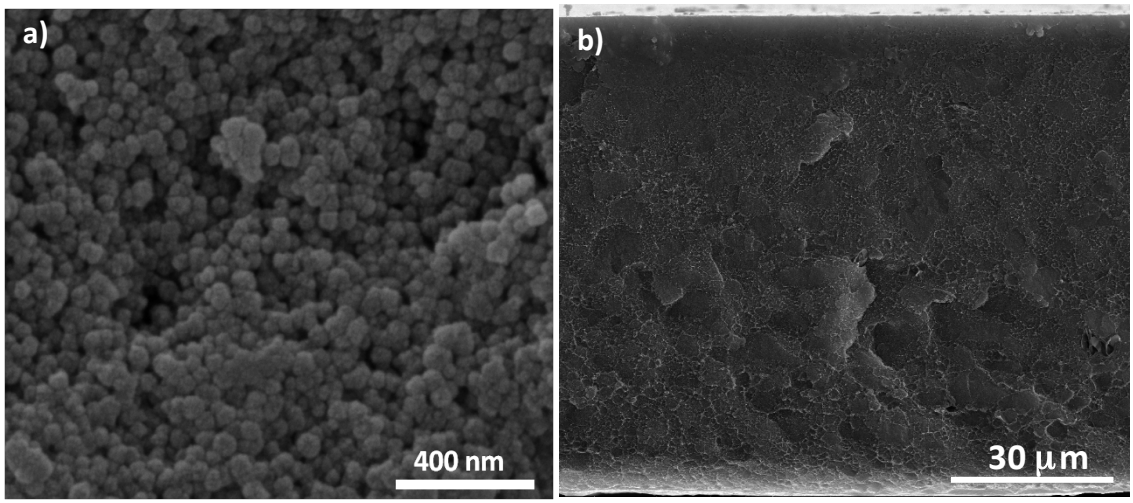

Figure 2. SEM photographs: a) MIL-101(Cr) particles; b) MIL-101(Cr)-PI MMM.

The nitrogen adsorption-desorption isotherm from the MIL-101(Cr) powder (Fig. 3) corresponds to a type IV isotherm. The step at P/P_0=0.2 corresponds to the mesopores of MIL-101(Cr). There is a hysteresis loop between the adsorption and desorption curves at P/P_0 between 0.8-1 due to the physisorbed nitrogen on the outer surfaces of the MIL-101(Cr) nanoparticles [49]. A BET specific surface of 2306 m^2/g was obtained, similar to previously reported data [46].

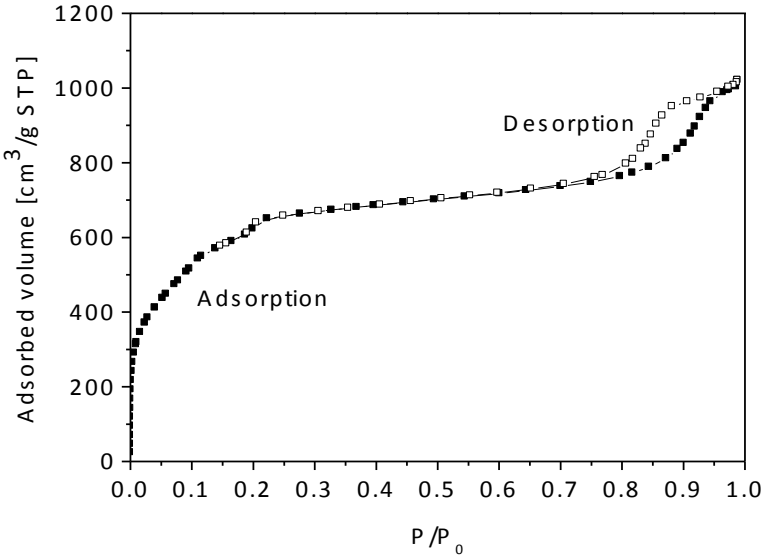

Figure 3. Nitrogen adsorption-desorption isotherm for as made MIL-101(Cr).

3.2. Membrane characterization

Membranes prepared with a theoretical 20 wt% of MIL-101(Cr) loading provided a homogeneous distribution of MOF particles across all the membrane thickness (87.8 ± 0.8 μm) with no sedimentation of MOF during the membrane drying, as can be observed in Fig. 2b. The preparation of MMMs with 30 wt% loading of MOF (not shown) was also carried out, since they were expected to have a better performance in the separation of water, as in the case of HKUST-1 [16]. However, these higher loading MMMs were broken during handling due to their extreme brittleness.

X-ray diffraction peaks of MIL-101(Cr)-PI (shown in Fig. 1) match those of as-synthesized MIL-101(Cr) and the simulated pattern, indicating the presence of MIL-101(Cr) in the MMM. In addition, this suggests that the structure of the MIL-101(Cr) particles was not affected during the preparation of the membrane.

The ATR-FTIR spectra of the pure PI, as-synthesized MIL-101(Cr) powder and MIL-101(Cr) MMMs, before and after esterification, can be observed in Fig. 4. The PI characteristic absorbance peaks are present in the MMMs spectra, where the peak at 1720 cm^{-1} corresponds to the symmetric and asymmetric stretching of the C=O groups in the imide, and those at 1510 and 1485 cm^{-1} are related to aromatic stretching of the para-disubstituted phenyl groups. In addition, the characteristic absorbance peaks of MIL-101(Cr), namely at 1420 cm^{-1} and 1620 cm^{-1} corresponding to COO^- stretching vibration symmetric and asymmetric, respectively [50, 51], can be observed in the MMM spectra both before and after the esterification reaction. In agreement with the XRD analyses, these results confirm the presence of unaltered MOF in the membranes.

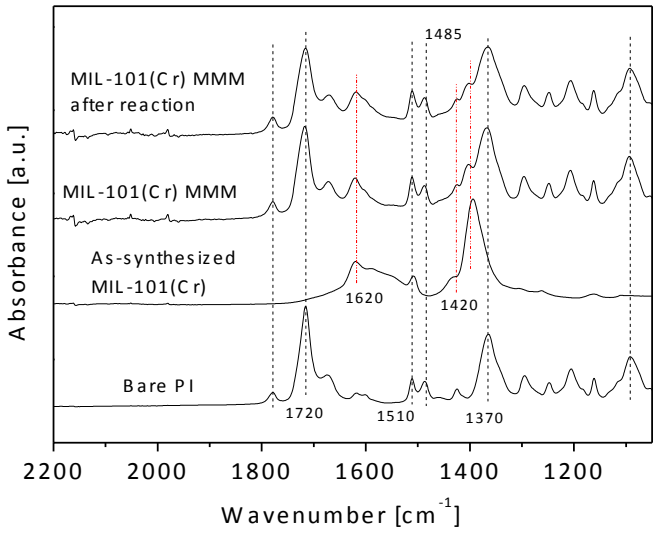

Figure 4. FTIR spectra of as-synthesized MIL-101(Cr) powder, PI membrane and MIL-101(Cr) MMMs: as-synthesized and after esterification reaction.

The TGA curves of different samples are depicted in Fig. 5. The amount of Cr can be determined from the curve of as-synthesized MIL-101(Cr) powder. After heating the sample up to 750 °C, 25.8 wt% of the sample still remains. This value is attributed to the oxidation of Cr to Cr_2O_3 [52], then the MIL-101(Cr) sample contained 18.0 wt% of Cr. This value is close to the theoretical amount of Cr in MIL-101(Cr) (13.3 wt%), according to the MIL-101(Cr) formula $(Cr_3O(OH)(H_2O)_2[C_6H_4(CO_2)_2]_3 \cdot 25H_2O)$ [52]. In the case of as-synthesized MMM, 4.6 wt% of sample still remains after heating. Comparing data from MIL-101(Cr) powder and from the corresponding MMM, the membrane contains 18.0 wt% of filler, which is near to the nominal 20 wt% used for the synthesis. It is worth noting that the addition of the MOF into the polymer matrix decreased the stability of the membrane from 480 °C for pure PI to 355 °C for the corresponding MMM, the temperature at which the degradation of the organic ligand of the

filler took place. This change in polymer stability can be attributed to the fact that the inorganic components of the MOF catalyze the polymer degradation [53].

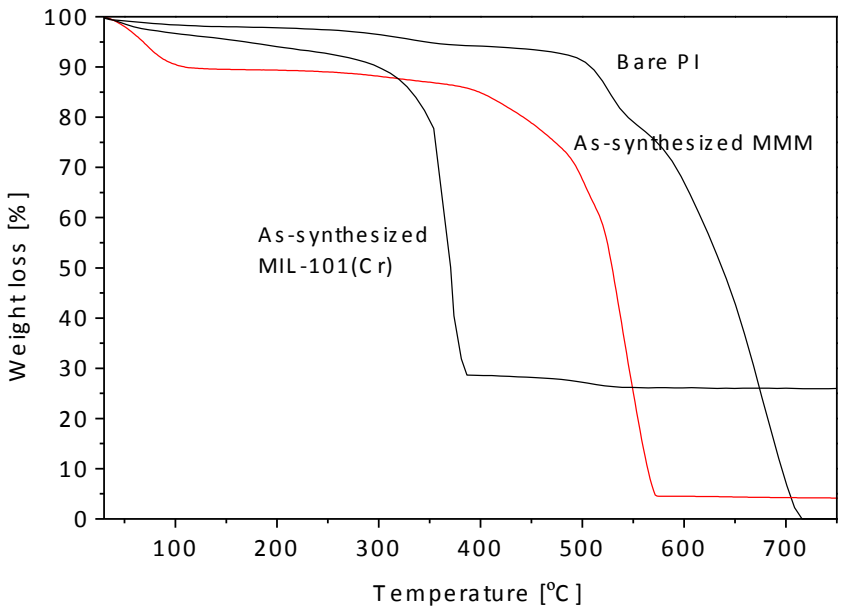

Figure 5. TGA curves of bare PI, as-synthesized MIL-101(Cr) powder and as-synthesized MIL-101(Cr)-PI MMM.

The water uptake of membranes with a 20 wt% loading of MIL-101(Cr) put in contact with water was determined to study the hydrophilicity of the membrane, since this affects its ability for water separation in the esterification reaction medium. The water uptake for membranes with 20 wt% of MIL-101(Cr) was 15.8 ± 1.6 wt% while the water uptake for a pure Matrimid® membrane was 2.5 wt%. This result indicates that the presence of hydrophilic MIL-101(Cr) particles enhances the water sorption into the membrane.

3.3. Esterification results

The experimental results obtained from esterification experiments at 70 °C are summarized in Table 1. The MIL-101(Cr)-PI membrane reactor reached a conversion of 70.5 %, clearly overtaking the conversion obtained with FBR, and slightly below the equilibrium conversion at the working temperature determined by Aspen HYSIS® (72.2 %). Although the HKUST-1-PI membrane reactor offered slightly higher conversion (71.8 %), the MIL-101(Cr)-PI membrane reactor performance was comparable to that of HKUST-1-PI and was more stable, as will be shown below.

Even though HKUST-1-PI MMM is more selective towards water, as can be observed from the molar fraction of water in permeate represented in Fig. 6b, the higher total permeate flux of MIL-101(Cr)-PI MMM (0.40 kg/(m^2·h) versus 0.26 kg/(m^2·h) for HKUST-1-PI) provided a value of water separated similar to that of HKUST-1-PI (0.15 kg/m^2·h for MIL-101(Cr)-PI versus 0.18 kg/m^2·h for HKUST-1-PI). This low difference in permeated water could also explain the slight difference between conversions. The higher total permeate flux of MIL-101(Cr)-PI MMM in comparison with HKUST-1-PI MMM could be explained by the higher porosity of the MIL-

101(Cr). In addition, its greater pore size (pore/cavities of 1.2/2.9 nm and 1.6/3.4 nm [52] as compared to 0.6/0.9x0.9 nm for HKUST-1[54]) made MIL-101(Cr)-PI MMM less selective than HKUST-1-PI MMM.

In the case of the PI membrane reactor, the low permeate flux of the PI membrane (0.105 $kg/m^2 \cdot h$) in comparison with those of MMMs is the reason for the low amount of water separated from the reaction medium (water flux in permeate of 0.07 $kg/m^2 \cdot h$). This low water removal from the system provided a low conversion of 63.5 %, scarcely reaching the conversion of the fixed bed reactor. Overall, the introduction of MOFs as fillers improved the water flux of membrane thus enhancing reactor performance.

The data of the water permeation flux, the water permeated/water produced in reaction ratio and the products/reactants separation factor are in good agreement. Even though the PI membrane is highly selective, showing the highest separation factor, its permeability is low, as the permeate total flux indicates. The PI membrane can only separate 30.2% of the water produced, which is not enough to improve the conversion. However, the MIL-101(Cr)-PI and HKUST-1-PI MMMs are able to separate 54% and 69% of the produced water, increasing the esterification reaction conversion. In addition, in spite of the fact that the MIL-101(Cr)-PI MMM permeates less water, it also separates ethyl acetate (see the molar fraction of ethyl acetate in the permeate represented in Fig. 6a) which contributes to the performance of the membrane reactor and can be related to the greater porosity of MIL-101(Cr) as compared to that of HKUST-1.

Table 1. Results of esterification experiments: average of data and standard deviation for steady state conversion stages. Experimental conditions: T= 70 °C; WHSV= 1.5 h^{-1}.

	MIL-101(Cr)-PI MR	**HKUST-1-PI MR**	**PI MR**	**FBR**
Conversion (%)	70.5 ± 0.6	71.8 ± 0.4	63.5 ± 0.3	63.7 ± 0.6
Permeate total flux ($kg/(m^2 \cdot h)$)	0.40 ± 0.01	0.26 ± 0.01	0.11 ± 0.00	---
Permeate water flux ($kg/(m^2 \cdot h)$)	0.15 ± 0.01	0.18 ± 0.02	0.07 ± 0.00	---
$H_2O_{permeated}$ /$H_2O_{produced}$ (%)	54 ± 1	69 ± 3	30 ± 5	---
S.F. prod /react	1.8 ± 0.1	2.5 ± 0.5	3.9 ± 0.1	---

The variations in the permeate total flux and molar fractions in the permeate during the esterification experiment carried out with MIL-101(Cr)-PI and HKUST-1-PI MMMs are depicted in Fig. 6. In the case of HKUST-1-PI the molar fraction of water in the permeate is higher than for MIL-101(Cr)-PI because of its higher selectivity towards water, as mentioned above. However, this molar fraction decreases during the experiment at the same time that the molar fraction of ethanol and acetic increase, indicating the loss of reactants. This indicates that the HKUST-1-PI membrane deteriorated during the experiment. In spite of the lower selectivity of MIL-101(Cr)-PI, the molar fractions in the permeate remained constant during the whole experiment, indicating a higher stability of the membrane. This would be expected given that MIL-101(Cr) is one of the most water-stable carboxylate MOFs [34], in contrast with the low

stability in water of HKUST-1 [55]. The different variation of the water molar fraction is in agreement with the deviation in the permeate water flux presented in Table 1 (0.01 kg/(m^2·h) for MIL-101(Cr)-PI and 0.02 kg/(m^2·h) for HKUST-1-PI).

To avoid the breakage of the HKUST-1-PI MMM that could damage the experimental setup, the esterification experiment with the HKUST-1-PI membrane reactor was stopped after 55 h. The conversion of this reactor remained constant in spite of the membrane deterioration due to its high selectivity. The experiment carried out with the MIL-101(Cr)-PI membrane reactor lasted for 77 h giving rise to constant molar fractions in the permeate, permeate flux and conversion, indicating a high stability of the MIL-101(Cr)-PI MMM.

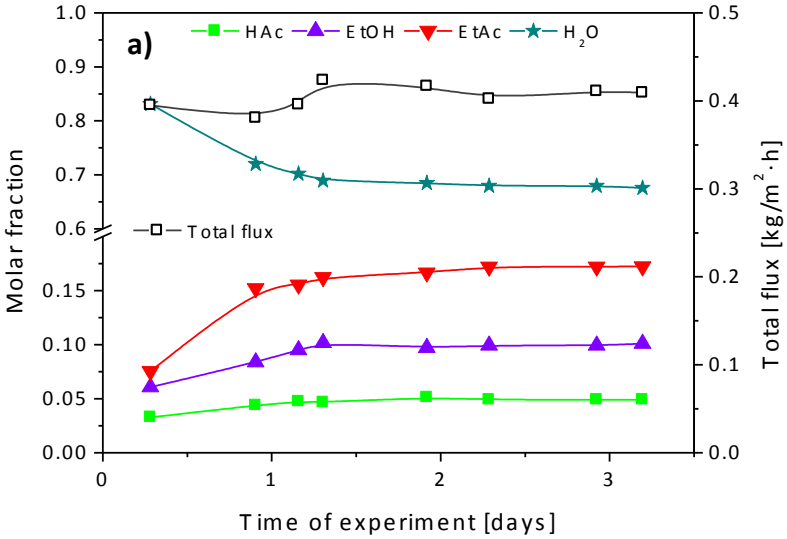

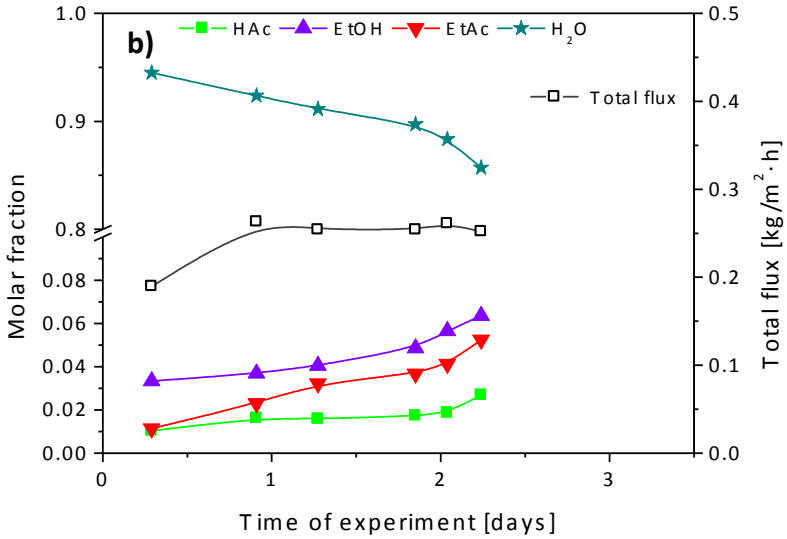

Figure 6. Molar fractions in permeate and total permeation flux as a function of time: a) MIL-101(Cr)-PI MR; b) HKUST-1-PI MR. Experimental conditions: T= 70 °C; WHSV= 1.5 h^{-1}.

3.4. Membrane stability after esterification

To gain further insight into the stability of MMMs, MIL-101(Cr)-PI MMM was characterized after the esterification experiments. No significant differences were observed either in the XRD (Fig. 1) or in the FTIR (Fig. 4) before and after the reaction experiments.

Fig. 7 shows SEM images of MIL-101(Cr)-PI and HKUST-1-PI MMMs before and after the esterification experiments. In the case of the MIL-101(Cr)-PI membrane (Fig. 7a and b), a homogeneous dispersion of MIL-101(Cr) particles can be observed even after reaction. Furthermore, there was no significant reduction in particle size that could be attributed to the partial dissolution or leaching of MIL-101(Cr) during the esterification (59 ± 7 nm before and 59 ± 9 nm after reaction). In the case of the HKUST-1-PI MMM (Fig. 7c and d), a degradation of HKUST-1 particles can be observed, which could explain the damage suffered by the HKUST-1-PI MMM during the esterification experiments.

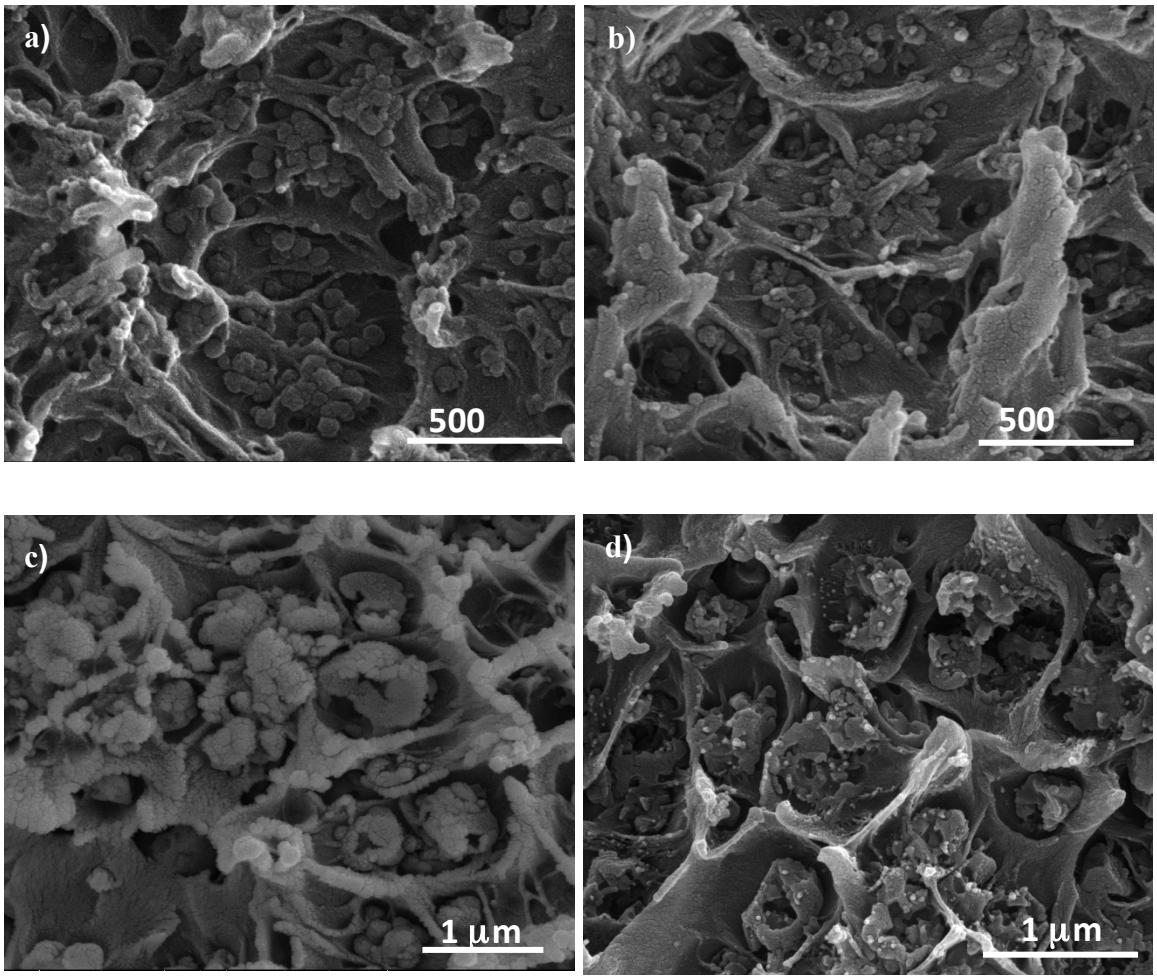

Fig. 7. SEM images of MMMs before (left) and after (right) esterification experiments: a) and b) MIL-101(Cr)-PI 20 wt% MMM; c) and d) HKUST-1-PI 30 wt% MMM.

For an in-depth study into the stability of MOFs during esterification, MIL-101(Cr)-PI 20 wt% and HKUST-1-PI 30 wt% MMMs were submitted to a leaching experiment. The membranes were left for 4 days in contact with a liquid mixture with all the components of the reaction.

TGA were carried out before and after the experiment (see Fig. 8) to determine the variation of metal in the MMM.

For the MIL-101(Cr)-PI MMM, the amount of metal (Cr) calculated by TGA remained constant during the leaching experiment. For the HKUST-1-PI MMM, the amount of metal (Cu) was reduced by 26%. These results are consistent with the differences observed between the MIL-101(Cr)-PI and HKUST-1-PI in the esterification results (Fig. 6) and SEM images (Fig. 7).

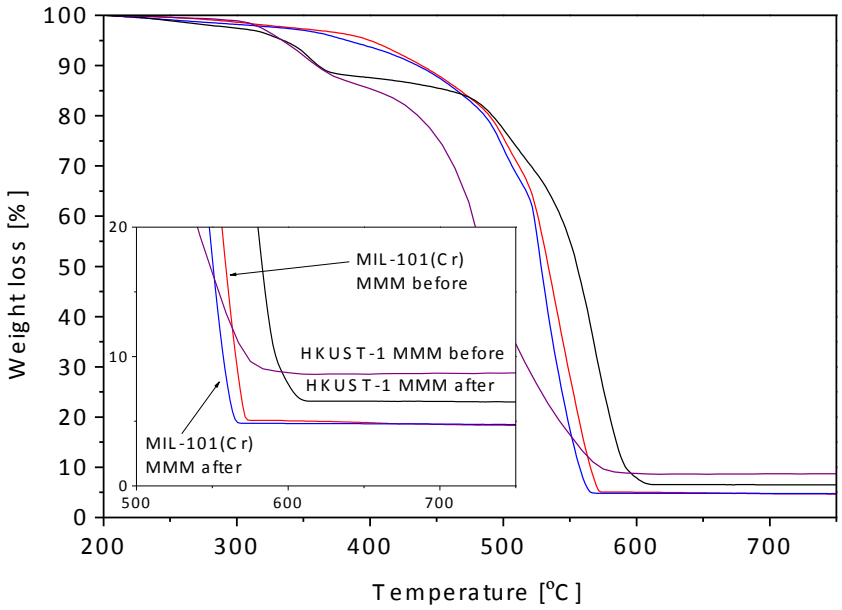

Fig. 8. TGA curves of MIL-101(Cr) and HKST-1 MMMs before and after leaching experiment.

4. Conclusions

Mixed matrix membranes (MMMs) based on the polyimide Matrimid® with MIL-101(Cr) as a porous nanostructured filler were successfully synthesized. MIL-101(Cr)-PI and HKUST-1-PI MMMs were applied to a membrane reactor for the esterification of acetic acid with ethanol. The presence of MOF as filler improved the membrane permeation flux, which produced higher conversions than in the case of a pristine polymeric membrane. Even though HKUST-1-PI is more selective towards water, the higher permeation flux of MIL-101(Cr)-PI provides a reactor performance comparable to that of HKUST-1-PI. Furthermore, MIL-101(Cr)-PI MMM exhibited a higher stability to the reaction medium than HKUST-1-PI MMM, maintaining constant molar fractions in permeate, conversion and permeation flux for more than 3 days. The difference in stability of MIL-101(Cr)-PI and HKUST-1-PI MMMs was confirmed by the characterization of the membranes after reaction experiments and by leaching experiments (SEM and TGA). Finally, MIL-101(Cr)-PI MMMs are promising materials for use in membrane reactors for esterification reactions, with a performance comparable to other MMMs with MOFs as filler, and with greater stability.

Acknowledgements

Financial support from the Spanish Ministry of Economy and Competitiveness (project MAT2013-40556-R), the Regional Government of Aragon and the ESF is gratefully acknowledged.

The authors would like to acknowledge the University of Zaragoza for the use of the Servicio General de Apoyo a la Investigación-SAI and the Laboratorio de Microscopías Avanzadas (LMA) at INA.

References

[1] T. Uragami, J. Kishimoto, T. Miyata, Membrane reactor for acceleration of esterification using a special ionic liquid with reaction and separation and microwave heating, Catal. Today 2012, 193, 57-63.

[2] B. Sarkar, S. Sridhar, K. Saravanan, V. Kale, Preparation of fatty acid methyl ester through temperature gradient driven pervaporation process, Chem. Eng. J. 2010, 162, 609-615.

[3] X.H. Ma, H.X. Zhang, S.W. Gu, Y. Cao, X. Wen, Z.H. Xu, Process optimization and modeling of membrane reactor using self-sufficient catalysis and separation of difunctional ceramic composite membrane to produce methyl laurate, Sep. Purif. Technol. 132 (2014) 370–377.

[4] P. Mäki-Arvela, T. Salmi, M. Sundell, K. Ekman, R. Peltonen, J. Lehtonen, Comparison of polyvinylbenzene and polyolefin supported sulphonic acid catalysts in the esterification of acetic acid, Appl. Catal. A-Gen. 184 (1999) 25-32.

[5] J. Jafar, P.M. Budd, R. Hughes, Enhancement of esterification reaction yield using zeolite - A vapour permeation membrane, J. Membrane Sci. 199 (2002) 117–123.

[6] Ullmann's Encyclopaedia of Industrial Chemistry "Esters", vol. A9, 5th ed., Verlag, Chemie, Weinheim, 1985.

[7] J.C. Charpentier, In the frame of globalization and sustainability, process intensification, a path to the future of chemical and process engineering (molecules into money), Chem. Eng. J. 134 (2007) 84-92.

[8] N. Diban, A.T. Aguayo, J. Bilbao, A. Urtiaga, I. Ortiz, Membrane reactors for in situ water removal: a review of applications, Ind. Eng. Chem. Res. 52 (2013) 10342–10354.

[9] K.C. Wu, Y.W. Chen, An efficient two-phase reaction of ethyl acetate production in modified ZSM-5 zeolites, Appl. Catal. A-Gen. 257 (2004) 33–42.

[10] S.R. Kirumakki, N. Nagaraju, K.V.R. Chary, Esterification of alcohols with acetic acid over zeolites H beta, HY and HZSM-5, Appl. Catal. A-Gen. 299 (2006) 185–192.

[11] T.A. Peters, N.E. Benes, A. Holmen, J.T.F. Keurentjes, Comparison of commercial solid acid catalysts for the esterification of acetic acid with butanol, Appl. Catal. A-Gen. 297 (2006) 182–188.

[12] O. de la Iglesia, R. Mallada, M. Menéndez, J. Coronas, Continuous zeolite membrane reactor for esterification of ethanol and acetic acid, Chem. Eng. J. 131 (2007) 35-39.

[13] K.C.S. Figueiredo, V.M.M. Salim, C.P. Borges, Synthesis and characterization of a catalytic membrane for pervaporation-assisted esterification reactors, Catal. Today 809 (2008) 133−135.

[14] A. Hasanoğlu, Y. Salt, S. Keleşer, S., Dincer, The esterification of acetic acid with ethanol in a pervaporation membrane reactor, Desalination 245 (2009) 662–669.

[15] P. Delgado, M.T. Sanz, S. Beltrán, L.A. Núñez, Ethyl lactate production via esterification of lactic acid with ethanol combined with pervaporation, Chem. Eng. J. 165 (2010) 693–700.

[16] S. Sorribas, A. Kudasheva, E. Almendro, B. Zornoza, O. de la Iglesia, C. Téllez, J. Coronas, Pervaporation and membrane reactor performance of polyimide based mixed matrix membranes containing MOF HKUST-1, Chem. Eng. Sci. 124 (2015) 37-44.

[17] E. Sert, F.S. Atalay, Butyl acrylate production by esterification of acrylic acid withn-butanol combined with pervaporation, Chem. Eng. Process. 81 (2014) 41–47.

[18] W. Zhang, S. Na, W. Li, W. Xing, Kinetic Modeling of Pervaporation Aided Esterification of Propionic Acid and Ethanol Using T Type Zeolite Membrane, Ind. Eng. Chem. Res. 54 (2015) 4940−4946.
[19] J. Caro, M. Noack, P. Kolsch, Zeolite membranes: from the laboratory scale to technical applications, Adsorption 11 (2005) 215–227.
[20] S. Khajavi, J.C. Jansen, F. Kapteijn, Application of a sodalite membrane reactor in esterification—coupling reaction and separation, Catal. Today 156 (2010) 132-139.
[21] D. Hua, T.S. Chung, Universal surface modification by aldehydes on polymeric membranes for isopropanol dehydration via pervaporation, J. Membrane Sci. 492 (2015) 197-208.
[22] S. Korkmaz, Y. Salt, S. Dincer, Esterification of acetic acid and isobutanol in a pervaporation membrane reactor using different membranes, Ind. Eng. Chem. Res. 50 (2011) 11657–11666.
[23] P.P. Lu, Z.L: Xu, X.H. Ma, Y. Cao, Preparation and characterization of perfluorosulfonic acid nanofiber membranes for pervaporation-assisted esterification, Ind. Eng. Chem. Res. 52 (2013) 8149−8156.
[24] A.P. Rathod, K.L. Wasewar, C.K. Yoo, Enhancement of esterification of propionic acid with isopropyl alcohol by pervaporation reactor, J. Chem. (2014), Article ID 539341, 4 pages.
[25] X. Zhan, J. Lu, T. Tan, J. Li, Mixed matrix membranes with HF acid etched ZSM-5 for ethanol/water separation: preparation and pervaporation performance, Appl. Surf. Sci. 259 (2012) 547–556.
[26] D.P. Suhas, T.M. Aminabhavi, A.V. Raghu, Mixed matrix membranes of H-ZSM5-loaded poly(vinyl alcohol) used in pervaporation dehydration of alcohols: influence of silica/alumina ratio, Polym. Eng. Sci. 54 (2014) 1774-1782.
[27] B. Baheri, M. Shahverdi, M. Rezakazemi, E. Motaee, T. Mohammadi, Performance of PVA/NaA mixed matrix membrane for removal of water from ethylene glycol solutions by pervaporation, Chem. Eng. Commun. 202 (2015) 316-321.
[28] J.N. Shen, Y.X. Chu, H.M. Ruan, L.G. Wu, C.J. Gao, B. Van der Bruggen, Pervaporation of benzene/cyclohexane mixtures through mixed matrix membranes of chitosan and Ag+/carbon nanotubes, J. Memb. Sci. 462 (2014) 160-169.
[29] S. Panahian, A. Raisi, A. Aroujalian, Multi layer mixed matrix membranes containing modified-MWCNTs for dehydration of alcohol by pervaporation process, Desalination 355 (2015) 45-55.
[30] S.D. Bhat, T.M. Aminabhavi, Novel sodium alginate composite membranes incorporated with SBA-15 molecular sieves for the pervaporation dehydration of aqueous mixtures of isopropanol and 1,4-dioxane at 30 °C, Micropor. Mesopor. Mat. 91 (2006) 206–214.
[31] A. Kudasheva, S. Sorribas, B. Zornoza, C. Téllez, J. Coronas, Pervaporation of water/ethanol mixtures through polyimide based mixed matrix membranes containing ZIF-8, ordered mesoporous silica and ZIF-8-silica core-shell spheres, J. Chem. Technol. Biot. 90 (2015) 669-677.
[32] B. Zornoza, C. Téllez, J. Coronas, J. Gascón, F. Kapteijn, Metal organic framework based mixed matrix membranes: an increasingly important field of research with a large application potential, Micropor. Mesopor. Mat. 166 (2013) 67–78.

[33] S. Basu, A. Cano-Odena, I.F.J. Vankelecom, MOF-containing mixed-matrix membranes for CO_2/CH_4 and CO_2/N_2 binary gas mixture separations, Sep. Purif. Technol. 81 (2011) 31–40.

[34] H.B.T. Jeazet, C. Staudt, C. Janiak, A method for increasing permeability in O_2/N_2 separation with mixed-matrix membranes made of water-stable MIL-101 and polysulfone, Chem. Commun. 48 (2012) 2140-2142.

[35] B. Seoane, C. Téllez, J. Coronas, C. Staudt, NH_2-MIL-53(Al) and NH_2-MIL-101(Al) in sulfur-containing copolyimide mixed matrix membranes for gas separation, Sep. Purif. Technol. 111 (2013) 72-81.

[36] C.H. Kang, Y.F. Lin, Y.S. Huang, K.L. Tung, K.S. Chang, J.T. Chen, W.S. Hung, K.R. Lee, J.Y. Lai, Synthesis of ZIF-7/chitosan mixed-matrix membranes with improved separation performance of water/ethanol mixtures, J. Membrane Sci. 438 (2013)105–111.

[37] Y. Li, L.H. Wee, J. Martens, I. Vankelecom, ZIF-71 as a potential filler to prepare pervaporation membranes for bio-alcohol recovery, J. Mater. Chem. A 2 (2014) 10034–10040.

[38] M. Amirilargani, B. Sadatnia, Poly(vinyl alcohol)/zeolitic imidazolate frameworks (ZIF-8) mixed matrix membranes for pervaporation dehydration of isopropanol, J. Membrane Sci. 469 (2014) 1-10.

[39] D. Hua, Y.K. Ong, Y. Wang, T. Yang, T.S. Chung, ZIF-90/P84 mixed matrix membranes for pervaporation dehydration of isopropanol, J. Membrane Sci. 453 (2014) 155–167.

[40] X.L. Liu, Y.S. Li, G.Q. Zhu, Y.J. Ban, L.Y. Xu, W.S. Yang, An organophilic pervaporation membrane derived from metal-organic framework nanoparticles for efficient recovery of bio-alcohols. Angew. Chem. Int. Ed. 50 (2011) 10636–10639.

[41] S.G. Adoor, L.S. Manjeshwar, S.D. Bhat, T.M. Aminabhavi, Aluminum-rich zeolite beta incorporated sodium alginate mixed matrix membranes for pervaporation dehydration and esterification of ethanol and acetic acid, J. Membrane Sci. 318 (2008)233–246.

[42] S.D. Bhat, T.M. Aminabhavi, Pervaporation-aided dehydration and esterification of acetic acid with ethanol using 4A zeolite-filled cross-linked sodium alginate-mixed matrix membranes, J. Appl. Polym. Sci. 113 (2009) 157-168.

[43] H.B.T. Jeazet, T. Koschine, C. Staudt, K. Raetzke, C. Janiak, Correlation of gas permeability in a metal-organic framework MIL-101(Cr)-polysulfone mixed-matrix membrane with free volume measurements by positron annihilation lifetime spectroscopy (PALS), Membranes 3 (2013) 331-353.

[44] M. Naseri, S.F. Mousavi, T. Mohammadi, O. Bakhtiari, Synthesis and gas transport performance of MIL-101/Matrimid mixed matrix membranes, J. Ind. Eng. Chem. 29 (2015) 249-256.

[45] G. Akiyama, R. Matsuda, H. Sato, A. Hori, M. Takata, S. Kitagawa, Effect of functional groups in MIL-101 on water sorption behavior, Micropor. Mesopor. Mat. 157 (2012) 89–93.

[46] N.A. Khan, I.J. Kang, H.Y. Seok, S.H. Jhung, Facile synthesis of nano-sized metal-organic frameworks, chromium-benzenedicarboxylate, MIL-101, Chem. Eng. J. 166 (2011) 1152-1157.

570 [47] L. H. Wee, M. R. Lohe, N. Janssens, S. Kaskel, J. A. Martens, Fine tuning of the metal-
571 organic framework $Cu_3(BTC)_2$ HKUST-1 crystal size in the 100 nm to 5 micron range, J.
572 Mater. Chem. 22 (2012) 13742-13746.
573 [48] A.A. Yakovenko, J.H. Reibenspies, N. Bhuvanesh, H.C. Zhou, Generation and applications
574 of structure envelopes for porous metal-organic frameworks, J. Appl. Crystallogr. 46
575 (2013) 346–353.
576 [49] D. Jiang, A.D. Burrows, K.J. Edler, Size-controlled synthesis of MIL-101(Cr) nanoparticles
577 with enhanced selectivity for CO_2 over N_2, Cryst. Eng. Comm. 13 (2011) 6916-6919.
578 [50] H. Mahdavi, L. Ahmadian-Alam, 32.Sulfonic acid functionalization of 2-
579 aminoterephthalate metal -organic framework and silica nanoparticles by surface initiated
580 radical polymerization: as proton-conducting solid electrolytes, J. Polym. Res. 22 (2015)
581 article number 67, 12 pages.
582 [51] F. Farzaneh, Y. Sadeghi, Immobilized V-MIL-101 on modified Fe3O4 nanoparticles as
583 heterogeneous catalyst for epoxidation of allyl alcohols and alkenes, J. Mol. Catal. A-Gen.
584 398 (2015) 275-281.
585 [52] G. Férey, C. Mellot-Draznieks, C. Serre, F. Millange, J. Dutour, S. Surblé, I. Margiolaki, A
586 chromium terephthalate-based solid with unusually large pore volumes and surface area.
587 Science 309 (2005) 2040-2042.
588 [53] F. Cacho-Bailo, S. Catalán-Aguirre, M. Etxeberría-Benavides, O. Karvan, V. Sebastian, C.
589 Téllez, J. Coronas, Metal-organic framework membranes on the inner-side of a polymeric
590 hollow fiber by microfluidic synthesis, , J. Membrane Sci. 476 (2015) 277–285.
591 [54] S.S.Y. Chui, S.M.F. Lo, J.P.H. Charmant, A.G. Orpen, I.D. Williams, A chemically
592 functionalizable nanoporous material $[Cu_3(TMA)_2(H_2O)_3]_n$, Science 283 (1999) 1148-1150.
593 [55] P. Kuesgens, M. Rose, I. Senkovska, H. Froede, A. Henschel, S. Siegle, S. Kaskel,
594 Characterization of metal-organic frameworks by water adsorption, Micropor. Mesopor.
595 Mat. 120 (2009) 325-330.